**EUROPEAN ORGANIZATION FOR NUCLEAR RESEARCH**
CERN — A&B DEPARTMENT

**CERN-AB-2008-030 BI**

# Model of Carbon Wire Heating in Accelerator Beam

**M. Sapinski**

CERN – Geneva - Switzerland

**Abstract**

A heat flow equation with beam-induced heating and various cooling processes for a carbon wire passing through a particle beam is solved. Due to equation nonlinearity a numerical approach based on discretization of the wire movement is used. Heating of the wire due to the beam-induced electromagnetic field is taken into account. An estimation of the wire sublimation rate is made. The model is tested on SPS, LEP and Tevatron Main Injector data. Results are discussed and conclusions about limits of Wire Scanner operation on LHC beams are drawn.
.

CERN-AB-2008-030
24 Jul 2008

Geneva, Switzerland
September, 2008

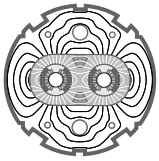

July 24, 2008

# Model of carbon wire heating in accelerator beam

Mariusz Sapinski *
CERN CH-1211 Geneva 23, Switzerland

Keywords: Wire Scanner, carbon fiber, beam heating

Summary

A heat flow equation with beam-induced heating and various cooling processes for a carbon wire passing through a particle beam is solved. Due to equation nonlinearity a numerical approach based on discretization of the wire movement is used. Heating of the wire due to the beam-induced electromagnetic field is taken into account. An estimation of the wire sublimation rate is made. The model is tested on SPS, LEP and Tevatron Main Injector data. Results are discussed and conclusions about limits of Wire Scanner operation on LHC beams are drawn.

*mail: mariusz.sapinski@cern.ch

# Contents

# 1 Introduction

Wire Scanners [1] are devices widely used in accelerators to measure the beam profile. They provide direct and accurate measurement with resolution down to 1 $\mu$m and they are considered as a reference for calibration of other instruments.

During the scan, the wire is moved through the beam with a constant velocity. It is heated by the electromagnetic coupling to the beam current [2]. After entering the beam it is irradiated, heated up and cooled down by heat transport along the wire, by thermal radiation and by thermionic emission. It might sublimate or even melt, depending on the beam conditions. The particles produced during the proton passage through the wire are measured in the detectors outside the vacuum pipe and based on their intensity the beam profile is reconstructed.

A variety of materials has been tested on the accelerator beams and carbon fibers has been find as the most resistant. Carbon fiber has a crystal structure of graphite with layers of atoms perpendicular to the wire axis. Most of the physical properties of the carbon fiber are the same as the graphite, but some, for instance Young's modulus or electric resistance, are fiber-specific.

The wire breakage has been observed many times with different beams. The cross-section of the broken wire has been photographed and analysed [3, 4]. These photographs indicate different breakage mechanism depending on beam conditions.

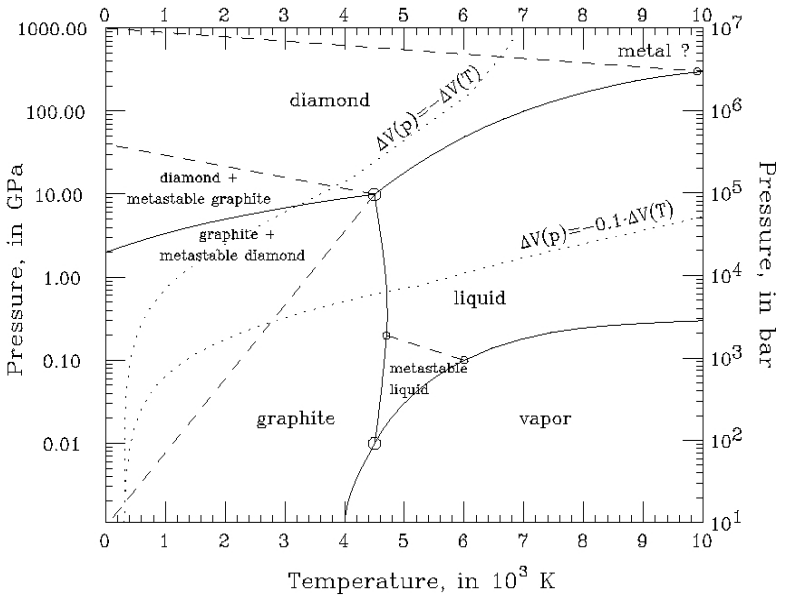


Figure 1: *Carbon phase diagram from [5].*

The mechanisms leading to the wire damage during the scan can be: brittle failure, plastic failure, sublimation, melting and thermal fatigue. In case of normal operation, when the wire breaks after thousands of scans, a combination of the above factors is relevant. For instance, as seen in some photographs in [3], the wire has

significantly sublimated before breaking. The sublimation removes the external part of the wire which contributes the most to its total strength, as it contains crystals which are more oriented then the ones in the core [6].

According to the carbon phase diagram, graphite cannot melt for pressures below 10 MPa. Despite of this, visual inspection of the broken wire with use of microscope show sometimes shapes similar to frozen drops [7]. It suggests that high pressures are achieved during the scan of the beam due to fast rise of temperature. At the same time, the rate of temperature raise during the scan of even very collimated LHC beam is slower than speed of sound therefore the thermal shock wave does not develop.

The LHC beam poses very demanding conditions for the wire. If scanning of the full beam would be possible the total energy deposited during a scan would be almost 2 J in a time of about 800 $\mu$s, therefore the instantaneous power released would reach 2 kW in a small part of less than 1 mm of the wire. No material can withstand such conditions.

The goals of this study are:

- determine the maximal temperature of the wire during the scan,
- attempt to estimate the conditions at which the wire breaks,
- determine the beam parameter range safe for operation of the Wire Scanner.

In order to answer above questions a model of wire heating by the beam and cooling has been created. The model has been implemented as a `root` macro. In addition simulations with use of Geant4 have been carried out in order to estimate the the proton energy deposition in a thin target. A simple toy model of wire sublimation and an estimation of the beam inductive heating complete the study.

This report is organized as follows. In Section 2, the model of energy flow in the wire is described. Section 3 presents studies about beam-induced energy deposit. Sections 5 to 7 present modelisation of cooling processes. Section 8 is devoted to heating due to electromagnetic induction from beam current. In Section 9, the sublimation process is addressed. Section 10 describes the results of the model for various beam conditions. Section 11 is devoted to the numerical stability of the algorithm and the report is concluded in Section 12.

# 2 Wire heating model

The temperature of a wire in a particle beam is described by Equation 1. The left side of the Equation represents heating of the wire by the beam and the right side represents the wire heat capacity and four cooling processes: radiation cooling ("graybody" radiation), heat transport along the wire, the thermionic cooling (together with re-heating by the current compensating thermionic current) and cooling due to sublimation. The Equation is discretized in time bins $\Delta$t and in wire slices

$\Delta$y. Every wire slice has position y and temperature T. The Equation 1 is written for a given slice.

$$\begin{aligned} E_{dep}\frac{\Delta N_{hits}}{\Delta t} &= \rho_C V c_p(T)\frac{\Delta T}{\Delta t} \\ &- A_{rad}\epsilon\sigma(T^4 - T_{amb}^4) - \lambda(T)A_d\frac{\Delta T}{\Delta y} \\ &- A_{rad}(\phi + \frac{2k_B T}{q_e})J_{th}(y) + C(y)\Delta R J_{th-tot}^2 \\ &- H_{sub}\frac{\Delta n}{\Delta t} \end{aligned} \quad (1)$$

The variables used in the Equation 1 are summarized in Table 1.

| **variable** | **description** |
|---|---|
| $E_{dep}$ | energy deposited by a proton |
| $\rho_C$ | graphite density |
| $c_p(T)$ | graphite specific heat in function of temperature (see left plot of Figure 2) |
| V | volume of a wire bin where energy balance is calculated |
| $A_{rad}$ | the surface of the wire which radiates heat |
| $\epsilon$ | the emissivity |
| $\sigma$ | Stefan-Boltzmann constant ($5.67 \cdot 10^{-12}$ $\frac{J}{s \cdot cm^2 \cdot K^4}$) |
| $T_{amb}$ | temperature of environment |
| $\lambda(T)$ | is the graphite thermal conductivity in a function of temperature (see right plot of Figure 2) |
| $A_d$ | wire cross-section $\pi d^2/4$ |
| $\frac{\Delta T}{\Delta y}$ | local temperature gradient along the wire |
| $k_B$ | Boltzmann constant ($1.38 \cdot 10^{-23}$ $\frac{J}{K}$) |
| $\phi$ | carbon work function per electron (in Volts) |
| $J_{th}$ | thermionic current surface density |
| $q_e$ | elementary charge ($1.602 \cdot 10^{-19}$ C) |
| C(y) | a fraction (between 0 and 1) of current compensating for thermionic emission and flowing through the wire in position y |
| $\Delta R$ | electric resistance of a bin of the wire |
| $J_{th-tot}$ | total thermionic current emitted from the wire |
| $H_{sub}$ | is the enthalpy of sublimation |
| $\Delta n$ | amount of material sublimated |

Table 1: Variables of the wire model.

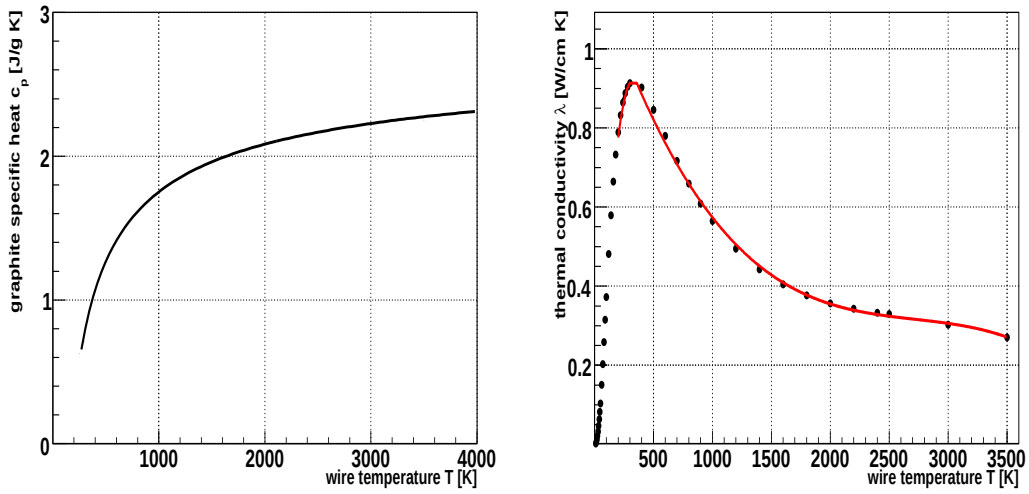


Figure 2: *Left plot: graphite specific heat as a function of temperature based on the data from [8]. Right plot: thermal conductivity of graphite as a function of temperature based on selected data from [9]; only the part above 250 K have been parametrized and used.*

As the Equation 1 is nonlinear due to dependence of carbon specific heat and thermal conductivity on the temperature and due to nonlinear form of the thermionic contribution, it must be solved numerically. Here a simple method based on discretization of time (ie. wire movement) and of position along the wire (y) has been used.

The wire is divided into slices(bins) along y-axis in order to correctly consider the heat transfer from hot center of the wire into colder edges. The choice of the bin size ($\Delta$y) along the wire length should depend on the beam size in that direction - it should be a fraction of the beam width ($\sigma_y$). The total wire length considered in the calculation is $6\sigma_y$. Initial temperature is set to 300 K or, in case of important coupling between the wire and the beam current, to a distribution along the wire (see Section 8).

The scanning process is divided into steps where during time $\Delta$t the wire moves by distance $\Delta$x. The natural choice of the time step $\Delta$t is the time which is needed for the wire to move by its diameter $d_{WS}$. In many cases such a time step is short enough to assure smooth variation of the wire temperature, but for narrow beams, as the one of LHC, a smaller step is used. Here the step was always small enough to assure that temperature change between two iterations in any wire bin(slice) is less than 10%.

The Equation 1 is typically solved from position $-3\sigma_x$ to $+3\sigma_x$. For every step the a calculation of every statement from Equation 1 is performed. For radiative and thermionic cooling, which depend very strongly on temperature, the temperature of the wire in a given step is estimated using first order Taylor expansion to the center of the time bin. This increases the accuracy of calculations.

# 3 Discussion of beam energy deposition

Every proton passing through the wire deposits a part of its energy. The dominant process is electronic energy loss. According to PDG [10] parametrization, the mean rate of electronic energy loss for protons of 450 GeV in carbon is about 2.5 MeV $cm^2/g$. For a carbon wire with density of $\rho_C = 2$ $g/cm^3$ and a diameter of $d_{WS} = 0.003$ cm the average energy deposited by a single proton is 15300 eV. For protons of 7 TeV this energy is by about 10-20% higher.

A Geant4 simulation has been carried out in order to correct the PDG estimations validity for a thin target. Geant4.9.0.p01 has been used with full electromagnetic physics model and QGSP hadronic physics model. The step size has been chosen to be 1 $\mu$m. Protons were shot in the direction of the wire center. The generated sample is 1 million of protons for every energy point: 450 GeV and 7 TeV.

The distribution of energy deposited in the wire ($E_{dep}$) is presented in Figure 3. The low energy part of the distribution has been fitted with Landau curve which is a good approximation in case of thin targets [11]. For 450 GeV beam the most probable value of the distribution is $6785 \pm 10$ eV and the mean value is 7640 eV, which is almost 2 times smaller than the value expected from the PDG. This discrepancy is interpreted as an effect of energy transfer to electrons which are knocked-off from the material (see for instance [12]). The spectra of particles emitted from the wire presented in Figure 4 are dominated by electrons.

The energy removed by electrons is subtracted from energy deposited in the target [13]. It is visible as a cutoff for energy of about 70 keV in the distribution of deposited energy in Figure 3 and as a maximum in the spectrum of emitted electrons.

The deposited energy spectrum has a tail at high energies. This tail is interpreted as an effect of nuclear interactions in the wire. It has been fitted with a gaussian curve in order to determine its mean value and approximate width. The mean value is $3.1 \pm 1.0$ MeV and the width is $\sigma = 3.9$ MeV. Events in the tail in average produce 16 secondary particles, while for low energy events the multiplicity of the secondaries is only 0.5.

The probability for a proton to generate a high energy deposit is about $2.2 \cdot 10^{-4}$ for 450 GeV beam and about $2.3 \cdot 10^{-4}$ for 7 TeV beam. This can be compared with Formula 2, which parametrizes the total proton-nuclei cross section [14]. This Formula is valid with 7% error in the HERA energy range from 150 to 920 GeV.

$$\sigma_{tot} = (52.86 \pm 0.23) \cdot A^{0.7694 \pm 0.0012} \text{ mb} = 209.8 \text{ mb} \tag{2}$$

Using Equation 3 (where: $m_A$ is carbon atomic mass, $N_A$ is Avogadro number) a probability of nuclear interaction is estimated to be about $7 \cdot 10^{-5}$. This value is 3 times smaller than the result of Geant4 simulation.

$$P = \sigma_{tot} \cdot \frac{\rho_C}{m_A} \cdot N_A \cdot d_{WS}, \tag{3}$$

The discrepancy is important, but the high energy tail is responsible for only 0.5%

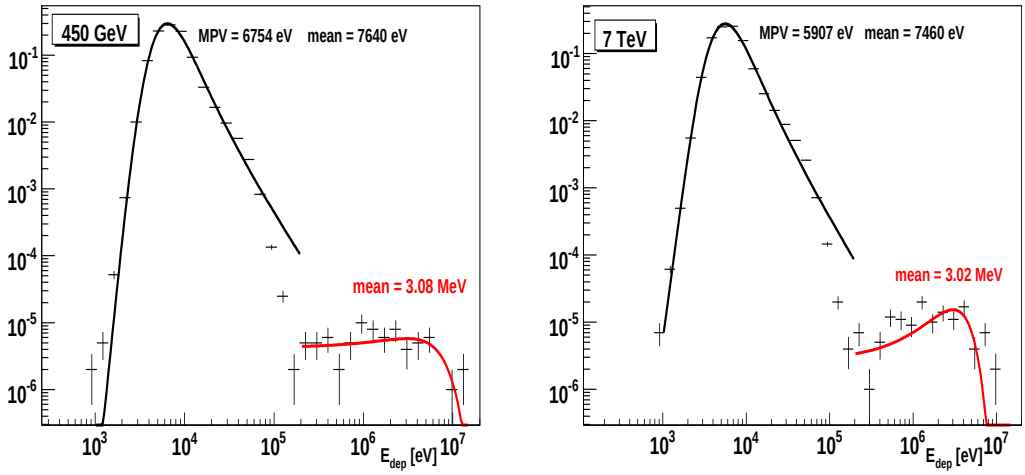


Figure 3: *The energy depositions in the wire from Geant4 simulation. Left plot: 450 GeV protons with low energy part fitted with Landau curve and high energy with gaussian. Right plot: the same for 7 TeV protons.*

of the total energy deposition. On the other hand, the effect of nuclear scattering of the protons is crucial for the study of the impact of the secondary particles on the coil of downstream magnets [15].

In the following calculations the value of energy deposited per proton ($\Delta$E in Equation 1) has been taken as the mean value of the distribution on the Figure 3. It is larger for 450 GeV protons (7640 eV) than for 7 TeV protons (7460 eV). It could be explained because for higher projectile momenta more energy escapes with knocked-off electrons [16]. But the parametrization of Bethe-Bloch equation for this energy range is an extrapolation from lower energies and has never been checked in an experiment. New processes should probably be included at this energy (muon-like bremsstrahlung and pair production).

The protons depositing energy in the wire pass not only through the center but also through peripheral part of the wire. To correct for the cylindrical shape of the wire, the total energy deposited is multiplied by a factor $\pi/4$.

In Table 2 a summary of different energy depositions per proton obtained in Geant4 simulations for various combinations of beam energy, wire diameter and carbon fiber density is presented. Every result has been obtained from a sample of 1 million of protons. Statistical errors of the mean deposited energy are also presented.

# 4 Wire breaking

The wire breakage has been observed many times on different beams. The cross-section of the broken wire has been photographed and analysed [3, 4]. From these

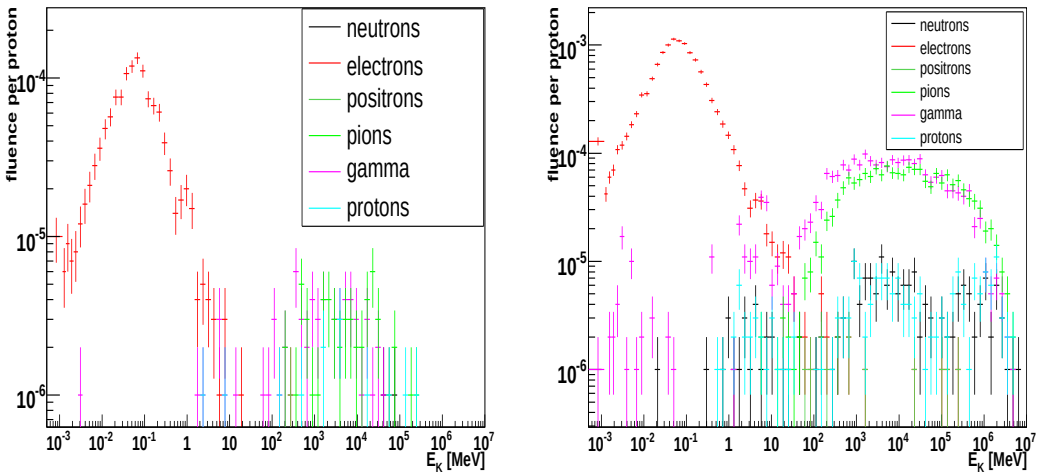


Figure 4: *The spectrum of particles emitted from the wire due to passage of a single 450 GeV (left plot) and 7 TeV (right plot) protons.*

photographs it can be concluded that the mechanism depends on the beam conditions. The most important parameters are the beam size, intensity and the duration of the beam pulses.

The mechanisms leading to the wire damage during the scan are the following:

- brittle failure: thermal stress and stress due to acceleration larger than the wire strength,
- plastic failure (rather not important as the carbon fiber is a brittle material),
- sublimation,
- melting,
- thermal fatigue.

In case of a normal operation, when the wire breaks after thousands of scans, the failure occurs due to thermal fatigue and sublimation. As an example on some photographs in [3], the wire is significantly sublimated in the location of breakage. The sublimation, described in Section 9, removes the external part of the wire which contributes the most to its total strength, as it contains crystals which are more oriented then the ones in the core [6]. The thermal fatigue, which leads to development of internal defects, also weakens the wire structure.

In SLAC Wire Scanners the wire breaking due to thermal stress concentration has been observed [4]. In this case the beam was made of dense and short bunches and wire heating due to a single bunch was very fast so the stress due to thermal expansion had no time to discharge via elastic waves along the wire. In case of LHC beams a single bunch does not deposit enough energy therefore the heating is less violent and the stress is discharged.

| accelerator | Energy [GeV] | $\rho_C$ [g/cm$^3$] | d [ $\mu$m] | $E_D$ [eV] |
|---|---|---|---|---|
| LHC | 7000 | 2.2 | 30 | $7551 \pm 105$ |
| LHC | 7000 | 2.0 | 30 | $7460 \pm 68$ |
| LHC | 7000 | 1.8 | 30 | $6804 \pm 66$ |
| LHC | 7000 | 1.8 | 10 | $2690 \pm 7$ |
| LHC | 450 | 2.0 | 30 | $7640 \pm 190$ |
| SPS | 450 | 2.0 | 30 | $7640 \pm 190$ |
| PS | 25 | 2.0 | 28 | $8517 \pm 117$ |
| Tevatron | 980 | 1.8 | 5 | $1193 \pm 27$ |
| Tevatron Main Injector | 120 | 1.8 | 33 | $7504 \pm 105$ |
| Tevatron Main Injector | 120 | 2.0 | 33 | $7732 \pm 79$ |

Table 2: *Values of energy deposits (mean values of deposited energy distributions) per proton obtained with Geant4 for different setups.*

The carbon fiber in the Wire Scanner is mounted on the fork and is prestressed with weight of about 50 g. This gives a constant tensile stress along the wire of about 700 MPa. When heated the wire expands. Assuming the thermal expansion coefficient increasing from 0% for room temperature to about 2% at 3800 K [17] and linear Hooke's law with typical elasticity modulus of 350 GPa [6] the compression stress neutralizes the prestress at temperature of about 2800 K.

The fiber compression strength is of the order of a few GPa, therefore the brittle failure of the fiber due to thermal expansion should happen for temperatures between 3000 K and 4000 K. The wire is accelerated and vibrates therefore a force transverse to the wire axis is applied. The fiber strength in this direction is much smaller than along the wire. A detailed analysis of stresses is a subject of a separate study [18].

In this report it is assumed that, in order to scan safely, the wire temperature should not exceed the one corresponding to safe scans on SPS ie. about 3600 K and the amount of the sublimated material should not exceed the one corresponding to the safe conditions ie. about 0.3% of the wire diameter. In case of LHC beams the maximum temperature condition is critical as the time of scan is so short that the sublimated material in negligible. The maximal wire temperature changes very fast with increase of the beam intensity therefore the safe beam intensities are estimated with relatively small uncertainty even if the critical temperature is not precisely known. These assumptions are rather conservative, but it is not taken into account that for high scan speeds the forces due to acceleration are larger and they might play role in the wire breaking.

It can be concluded that a proper choice of a carbon fiber is important for the wire durability. Particularly the fibers treated with high temperature during the carbonization phase of the production process have better mechanical properties. Also thin fibers which have better ratio of surface to volume have in general better mechanical properties.

# 5 Conductive cooling

Although the carbon thermal conductivity is high, the conductive cooling is expected to be small because of the small wire cross section. The thermal conductivity decreases with temperature (right plot of Figure 2). The time constant of conductive cooling depends on the local temperature gradient and is about 0.1 second as presented on the left plot of Figure 6. The green curve on this plot has been obtained by switching off the beam heating in the beam maximum and observing maximum temperature evolution due to a conductive cooling process.

The details of the implementation of the conductive cooling in the numerical solution are:

- The Fourier's law is used to calculate heat flowing in and flowing out of every cell of the wire.
- The temperature on the border ($T_b$) between bins along the wire length is calculated as an average of the temperature of the neighbor bins.
- The heat transfer due to conductivity is calculated for every bin:
  $\Delta Q_{ht} = \frac{\Delta t}{\Delta y}[\lambda(T_{b1})A_d(T - T_{i-1}) + \lambda(T_{b2})A_d(T - T_{i+1})]$,
  where $A_d$ is the wire cross section and $\lambda(T)$ is thermal conductivity.
- It is assumed that the heat leaks from the part of the wire included in the numerical calculations into the outside part - the temperature of the outside part is a linear extrapolation of the temperature distribution on the last 2 cells of the inside part (but it cannot be smaller than 300 K).

It can be concluded that the conductive cooling has a low impact on the temperature of the wire, because it is weak and it has a long time constant when compared to other cooling processes. Nevertheless, it plays an important role when the temperature is too low to make radiative cooling and thermoemission efficient.

The use of a material with much higher thermal conductivity as, for instance, carbon nanotubes [19] which have 20-100 times better thermal conductivity in room temperature than the carbon fiber, will not improve significantly the performance of the wire. This is mainly because the thermal conductivity decreases very fast with temperature and for the temperatures reached by the wire in the beam it becomes so low that the conductive cooling, as shown later, is negligible with respect to other cooling processes. In addition carbon nanotubes are expected to be unstable above 2500 K.

# 6 Radiative cooling

Radiative cooling is driven by Stefan-Boltzmann law. The heat radiated from the wire surface is proportional to the fourth power of the temperature. The difference

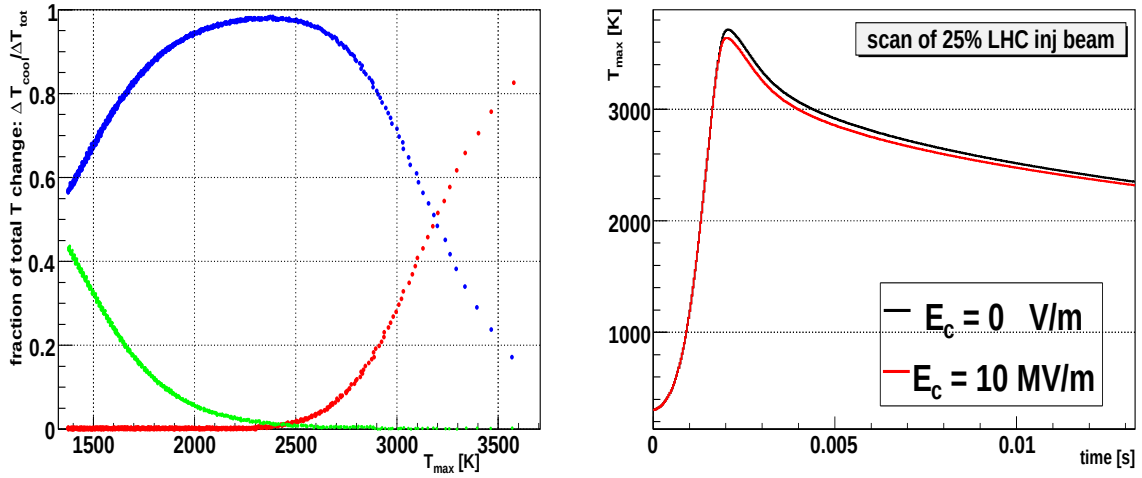


Figure 5: *Left plot: relative contribution of cooling processes to the total temperature change ($\Delta T_{tot}$) as a function of the maximum wire temperature. Blue points are for radiative cooling, red ones for thermionic and green are for the heat transfer. Right plot: the effect of enhancement of thermionic emission by external electric field.*

from the ideal black-body radiation is described by a factor called emissivity. The value found in literature [20] is about $0.8 \pm 0.05$ and depends weakly from temperature.

A strong dependence of the radiated energy from the temperature makes a numerical solution very sensitive to the size of the time bin. In order to stabilize the algorithm, the temperature in each step has been corrected using first order Taylor expansion: $\mathrm{T_{step}} = \mathrm{T_i} + \Delta\mathrm{t} \cdot \mathrm{T'_i}/2$, where $\mathrm{T'_i}$ is the first derivative of the temperature in time. The same correction has been used in case of thermionic cooling.

The time scale for radiation cooling can be estimated as:

$$\tau_{\mathrm{rad}} = \frac{\mathrm{c_p(T)m}}{\mathrm{A_{rad}}\epsilon\sigma} \int_{\mathrm{T_i}/2}^{\mathrm{T_i}} \frac{\mathrm{dT}}{\mathrm{T^4 - T_0^4}} \tag{4}$$

where $m$ is mass of a wire cell. This estimation gives around 44 milliseconds for 3267 K.

On the left plot of Figure 6 the blue line shows how the wire cools down due to radiation after stopping the beam heating. The time constant measured from this plot is about 20 ms for a temperature of 3267 K. The reason of this discrepancy is that the radiative cooling is described by a first-order linear time-invariant differential equation. Therefore, fitting radiative cooling with an exponential function is approximate.

# 7 Thermionic emission

Thermionic emission is an emission of electrons from a hot body caused by thermal energy. This phenomena increases violently with the wire temperature and becomes the dominant cooling process at high temperatures.

The density of the current emitted by the wire is described by Richardson-Dushman Equation 5.

$$\mathrm{J_{th}} = \mathrm{A_R} \cdot \mathrm{T}^2 \cdot \exp(-\frac{\phi}{\mathrm{k_B T}}) \tag{5}$$

where $\phi$ is the work function and $\mathrm{A_R}$ is Richardson constant, theoretically equal to:

$$\mathrm{A_R} = 4\pi \mathrm{mk}^2\mathrm{e/h}^3 = 120.173\ [\mathrm{Acm^{-2}K^{-2}}] \tag{6}$$

It is assumed here that the electrons are not coming back to the wire, ie. the charge which is leaving the wire is immediately compensated by the current flowing from the fork.

The power dissipated by thermionic current is:

$$\frac{\mathrm{dE_{th}}}{\mathrm{dt}} = \mathrm{A_{rad}}(\phi + \frac{2\mathrm{k_B T}}{\mathrm{q_e}})\mathrm{J_{th}} \tag{7}$$

The current compensating for charge loss due to thermionic emission, described in Equation 1 as $\mathrm{C(y)}\Delta\mathrm{R}\mathrm{J}^2_{\mathrm{th-tot}}$, is taken into account as an additional source of wire heating. $\mathrm{J_{th-tot}}$ is a total thermionic current emitted from the wire. The C(y) describes the thermoelectron flow from different locations along the wire. It is almost 0 in the center and 1 on the side of the wire, because all the current compensating for thermionic emission flows from the fork through the side of the wire while in the center only the fraction of it, which has not yet been dissipated, is preserved.

The resistance of the slice of the wire is expressed by Equation 8, where the $\sigma_{\mathrm{el}}$ is carbon electric resistivity assumed to be $10^{-3}$ $\Omega$ cm in room temperature and decreasing with temperature coefficient -0.0005 1/K.

$$\Delta\mathrm{R} = \sigma_{\mathrm{el}}\frac{\Delta\mathrm{y}}{\mathrm{A_d}} \tag{8}$$

This estimation is approximate but this heating source has a negligible impact on the final results.

The thermionic emission leads to a phenomena observed in Figure 10, where, for relatively wide beam, the temperature is almost stabilized at around 3500-3600 K during the time when the wire passes through the beam center. Instead of raising the temperature in the wire center, the hot zone spreads along the wire. The thermionic current emitted from the wire in this stage reaches about 0.17 A and the total charge emitted during this scan is $6 \cdot 10^{-3}$ Coulomb.

The time constant of the thermionic cooling is difficult to estimate analytically. On the left plot of Figure 6 the time constant for temperature 3330 K has been

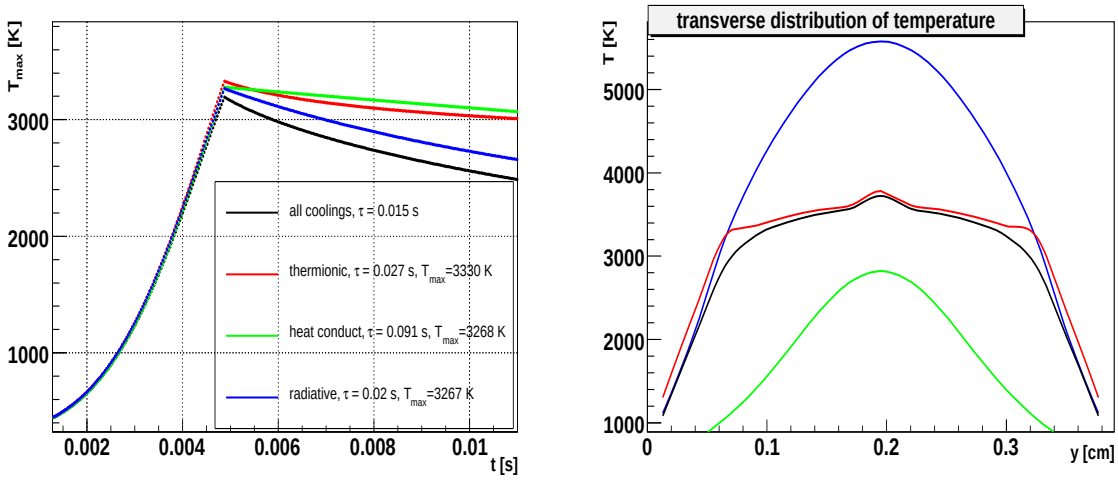


Figure 6: *Left plot: contribution of different cooling processes for scan with* $\mathrm{v} = 1$ m/s *and beam described in Section 10.1, which is stopped when the wire reaches the beam center. Red line - only thermionic cooling, green line - only conductive cooling, blue line - only radiative cooling, black line - all coo lings. The lines were obtained by switching off the beam when the wire reached the middle. Right plot: influence of cooling processes on the distribution of the temperature along the wire. It has been obtained with velocity of* $v = 10$ *cm/s and beam described in Section 10.1. Only for conductive cooling the beam intensity has been multiplied by 0.1 in order to fit the scale. The beam center is at y=0.2 cm. Threshold effect is visible for thermionic cooling at temperature of about 3400 K.*

estimated to be about 0.027 s, but it strongly depends on temperature and for 3900 K it is only 0.005 s.

The relative importance of cooling processes is summarized on the left plot of Figure 5. Up to about 1300 K the conductive cooling removes most of the heat. Above 1300 K the radiative cooling plays the main role, until about 3200 K when the thermionic cooling takes over.

The thermionic emission can be enhanced by the external electric field, as shown in Equation 9.

$$\mathrm{J_{th}} = \mathrm{A_R} \cdot \mathrm{T}^2 \cdot \exp(-\frac{\phi - \Delta \mathrm{W}}{\mathrm{k_B T}}) \tag{9}$$

The change of work function due to external field is described by Equation 10.

$$\Delta \mathrm{W} = \sqrt{\frac{\mathrm{q_e^3 E_c}}{4\pi\epsilon_0}} \tag{10}$$

and $\mathrm{E_c}$ is the field strength at the electrode expressed in V/m. The effect of the enhancement of the thermionic cooling by the external electric field is presented

on the right plot of Figure 5. The black curve shows evolution of the maximum temperature on the wire during the scan of 25% of the nominal beam at injection energy (see Section 10.3). The red curve shows the same but assuming additional electric field of 10 MV/m on the wire surface. This field strength is in the range of fields reached in modern RF cavities. The gain in cooling by thermionic emission is small.

# 8 Inductive heating from beam

The moving charges of the beam induce a current in the Wire Scanner elements. The coupling between the wire and the beam can be so strong that the wire might break even in the parking position as it happened in the SPS with LHC beam [2]. After this experience the RF-absorbing material has been fixed in the wire parking cavity what cured the wire breaking problem. Here it is assumed that the wire is well protected against the heating in its parking position and the RF-coupling to the beam starts only when the scan begins.

During the scan, as the wire approaches the beam, the dominant field component in the wire center is the field from the beam itself and not from image charges traveling on the walls of the vacuum chamber. The electric field value for the part of the wire which remains in the beam vicinity is expressed by Equation 11, which is a good approximation in case of a unbunched relativistic beam [21] with circular cross section. In case of a bunched beam the Equation is valid when the distance of the wire from the beam is smaller than the bunch length and when the longitudinal position of the wire and the bunch overlap, ie. when the bunch passes under the wire.

$$\mathrm{E} = \frac{1}{4\pi\epsilon_0}\frac{2\mathrm{Q}_{\mathrm{bunch}}}{\mathrm{l}_{\mathrm{bunch}}\mathrm{r}_{\mathrm{T}}} \tag{11}$$

In the space between bunches the electric field is negligible because of relativistic contraction of the field in the direction of motion.

On the left plot of Figure 7 the field configuration is shown. Only the field component along the wire $\mathrm{E_y}$ generates a current. The power released on the wire is proportional to $\mathrm{E_y^2}$, therefore the Figure explains the results presented on Figure 1 of [22] showing that the center of the wire, which upholds the direct beam impact, is not heated by RF-coupling to the beam.

It must be stressed that the interpretation of Figure 1 from [22] in terms of temperature is ambiguous. The luminosity function of the CCD camera used to register the wire temperature is unknown therefore even the conclusions about the shape of the temperature distribution must be drawn with caution as the temperature scale can be strongly nonlinear.

The spectra of the beam-generated fields are presented in Figure 7. The maximal frequencies $\mathrm{f_{LEP}} = 15$ GHz and $\mathrm{f_{LHC}} = 1.9$ GHz can be calculated from the bunch

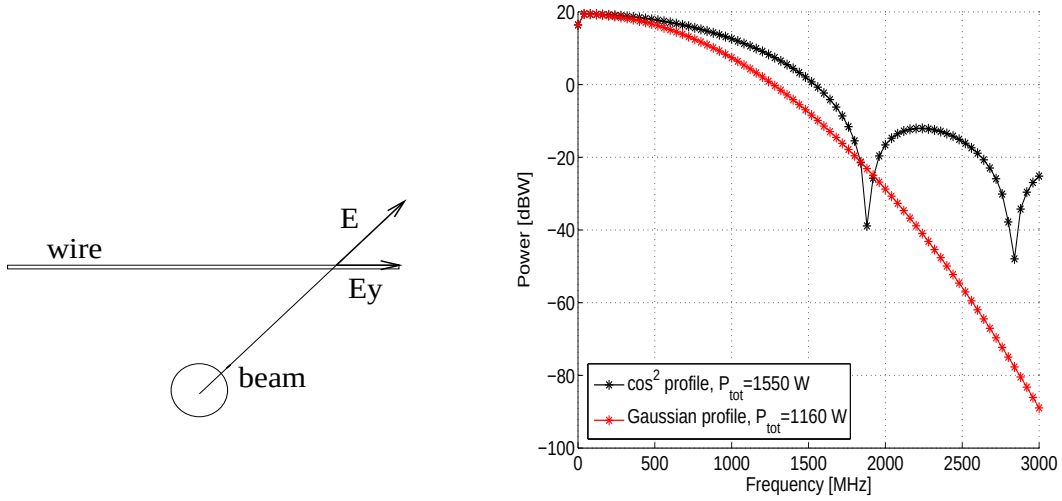


Figure 7: *Left plot: illustration of the electric field configuration on the wire approaching the beam. Right plot: The power in the harmonics of nominal LHC beam at top energy, 4$\sigma$ bunch length 1.06 ns. From SPS experience the Gaussian profile is believed to be more realistic. The plot is a courtesy of [23].*

length (see Table 3). But the dominant part of the power transmitted from the beam is in low frequency region therefore the skin effect can be neglected.

## 8.1 Comparison with LEP results

In the following, the report on wire breaking measurements in LEP [22] is used as a reference. The wire breakage due to RF-heating during the scan occured at beam current of a 6 mA. The beam parameters which affect RF-heating has been registered and the thermal radiation from the wire has been photographed with a CCD camera.

The parameters of LEP and LHC beams and the wires are presented in Table 3. The factor in the last column is an approximate estimation of how much more LHC beam heats up the wire with comparison to LEP beam. For instance the bunch in LHC is 7.7 times longer than in LEP. It means that every bunch spends 7.7 times more time to heat the wire, but as the bunch charge is similar in both machines, the current generated by LHC bunch will be $(7.7)^{-2}$ smaller and the temperature increase will be smaller than in LEP.

Summing up all the phenomena which affect the wire temperature during the RF-heating period it is found that full LHC beam is about 50 times safer than the LEP beam.

Therefore the wire breaking due to RF-coupling to the beam will happen at much higher beam densities than the breaking due to direct interaction with the beam. Nevertheless, for scans with 25% of LHC injection beam, described in Section 10.3,

| parameter | unit | LEP beam | LHC collision | LHC enhancement factor |
|---|---|---|---|---|
| particles in bunch $N_p$ | $\cdot 10^{11}$ | 1.0 | 1.1 | 1.21 |
| No of bunches | | 2x16 | 2808 | 88 |
| bunch length | cm | 1. | 7.7 | |
| duration of pulses | | | | 7.7 |
| beam current | | | | 0.017 |
| wire speed | cm/s | 25 | 100 | 0.25 |
| wire diameter | $\mu$m | 8 | 30 | |
| - therm. conductivity | | | | 0.07 |
| - heat capacity | | | | 0.07 |
| total | | | | 0.017 |

Table 3: *Values of beam parameters influencing the wire heating by electromagnetic induction.*

an initial distribution of the wire temperature has been assumed in order to take the RF-heating into account.

In the Table 3 it has been assumed that the beam acts as a current source. The total wire resistivity is about 400 $\Omega$ therefore it is very close to impedance of free space (377 $\Omega$) therefore it is not clear if the beam acts as a current source ($P \approx I^2_{beam} R$) or as voltage source ($P \approx U^2/R$). For the thinner LEP wire the second approximation is more adequate.

## 8.2 Simulation of the beam power loss on the wire

The intuitive picture presented in the previous Section has been confirmed by a simulation [23] using Ansoft HFSS. The relative loss as a function of wakefield frequency as presented on the left plot of Figure 8 has been convoluted with the beam spectrum, shown on the right plot of Figure 7.

The energy deposition has been used in the wire model which contain thermal conductivity. Other cooling processes are not adequate for the temperatures which are reached by the wire. On the right plot of Figure 8 the temperature evolution along the wire during the scan is presented. On the wire edges temperature raises from initial 300 K (at distance of 2cm from the beam) to almost 700 K (when wire crosses the beam). The temperature increase in the center of the wire is very small, what is confirmed by LEP measurements.

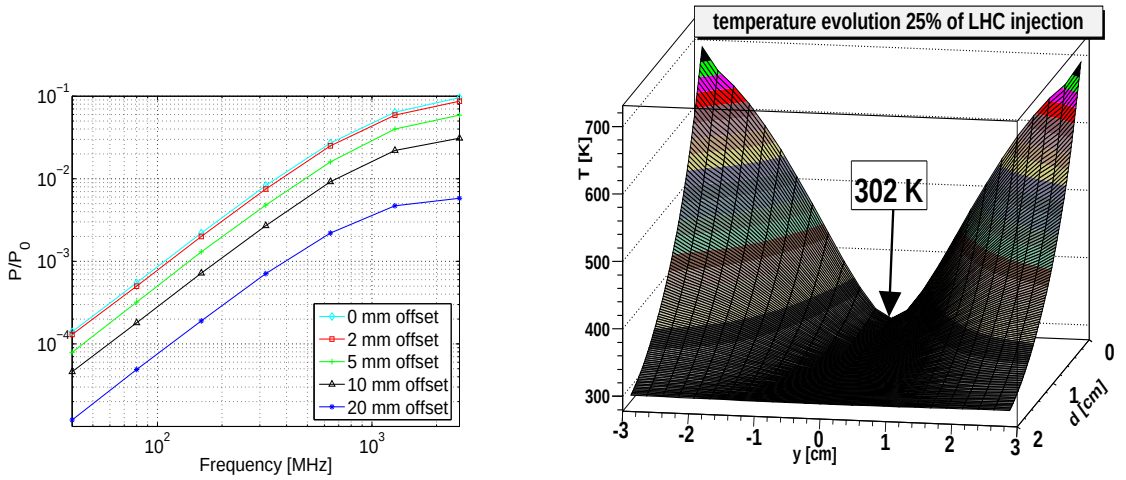


Figure 8: *Left plot: Total relative loss on the carbon wire as a function of beam spectrum frequency. The different curves are for various distances of the wire from the beam [23]. Right plot: The wire temperature evolution due to RF-heating. A 25% of LHC injection beam intensity is assumed.*

# 9 Estimation of wire sublimation rate

The wire sublimation rate has been estimated from a simple model [24]. It has been assumed that in a thin layer around the wire the carbon vapour pressure is in equilibrium with the wire material. This assumption means that the vapour pressure reaches its maximal value and, during the time $\Delta$t, no change of the pressure nor the temperature takes place. The beam scan is a process with a violent increase of the wire temperature therefore it is not an equilibrium process, but this assumption is conservative. The vapour pressure in non-equilibrium process would be smaller than the equilibrium one (carbon has no time to sublimate) and therefore less atoms would escape from the surface. In addition, during the cool-down, the vapour pressure becomes higher than the equilibrium pressure and re-sublimation happens. This two effects are not taken into account here.

The second important simplification of the calculations is the assumption that the carbon vapour is an ideal gas, therefore it does not have internal degrees of freedom linked to a rotation or an oscillation of the molecules. This assumption is also conservative as no energy escapes into these internal degrees of freedom therefore the average velocity of atoms is overestimated (Equation 14).

The vapour pressure data, presented on the left plot of Figure 9 and used in the calculations, have been obtained from [25]. The error on vapour pressure is large especially for high temperature where the sublimation takes place, and this constitutes an important source of uncertainty of the model.

The ideal gas law for the carbon vapour is presented in Equation 12, in which $p_{atm}$ is atmospheric pressure ($10^5$ Pa), $V_{mol} = 22.4$ dm$^3$ is the molar volume of ideal

gas in the standard temperature $\mathrm{T_{std}} = 273$ K.

$$\frac{\mathrm{p_{atm}} \cdot \mathrm{V_{mol}}}{\mathrm{T_{std}}} = \frac{\mathrm{p_{vap}} \cdot \mathrm{V_{vap}}}{\mathrm{T_{vap}}} \tag{12}$$

Hence, the carbon vapour density in the equilibrium layer can be expressed using the Formula 13.

$$\rho_{\mathrm{vap}} = \frac{\mathrm{m_{mol}}}{\mathrm{V_{mol}}} \frac{\mathrm{T_{std}}}{\mathrm{p_{atm}}} \frac{\mathrm{p_{vap}}(\mathrm{T_{vap}})}{\mathrm{T_{vap}}} \tag{13}$$

From the ideal gas theory the average velocity of gas particles (averaged over all directions in a hemisphere - factor $\frac{1}{2}$) is described by Formula 14.

$$v_{vap} = \frac{1}{2}\sqrt{\frac{8kT_{vap}}{m\pi}} \tag{14}$$

Using Equations 13 and 14 the amount of the sublimated material (the depth of the sublimated layer) in the time unit $\Delta$t can be expressed by Equation 15, where the factor $\frac{1}{2}$ comes from the fact that half of the particles have velocities in the direction of the wire surface.

$$d_{sub} = \frac{1}{2}\ v_{vap}\ \rho_{vap}\ \rho_C\ \Delta t \tag{15}$$

The Equation 15 is included in the program and the amount of sublimated material is subtracted from the wire in every time step $\Delta$t. Due to a strong dependence of the carbon vapour pressure from temperature, the total amount of sublimated material depends on the maximum temperature reached during the scan and the time the temperature is above critical. The removal of the material from the wire leads to decrease of the wire heat capacity and, as stated in Equation 1, cools down the wire because of sublimation heat, assumed to be 715 kJ/mole. The wire weight is about 130 $\mu$g and the amount of sublimated material is so small that the sublimation heat it is responsible for only about 1.5% degradation of the maximum temperature during the long scans.

On the right plot of Figure 9 the maximum temperature of the wire during the scan is compared to the decrease of wire radius due to sublimation. The sublimation process starts sharply at temperature of about 3300 K for the vapour pressure of a few Pa. Above that temperature the sublimation rate weakly depends on the temperature.

It is worth noticing that the SPS beam, which is wider, keeps the maximal wire temperature high for a longer time, leading to evaporation of more material than a fraction of the narrow LHC beam. In case of the LHC beam the breaking of the wire depends on the maximal temperature while in SPS beam the scan duration becomes important.

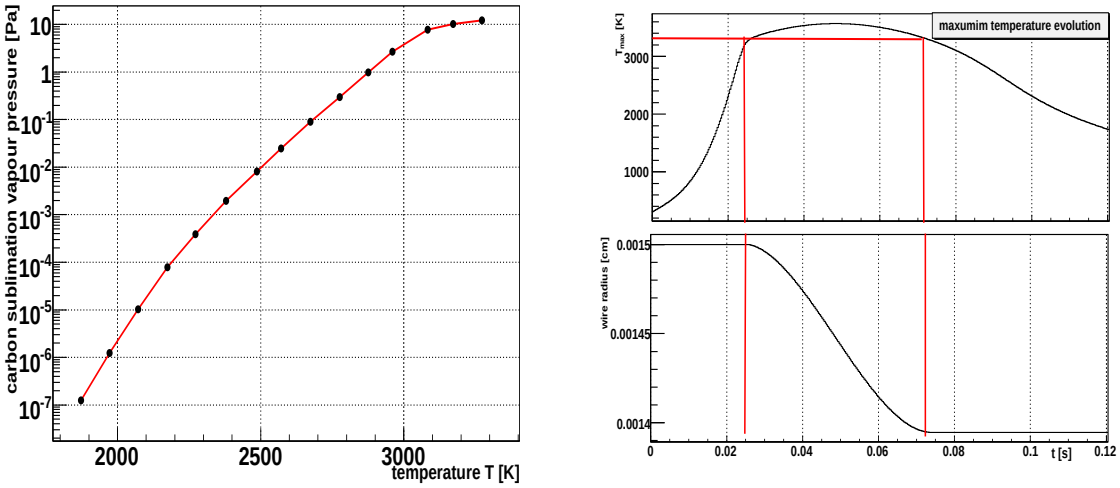


Figure 9: *Left plot: carbon vapour pression (in vacuum) as a function of the temperature. Right plot: illustration of the temperature evolution and corresponding decrease of the wire diameter in the sublimation model. The scan conditions are described in Section 10.1.*

It can be concluded that in order to assure safe operation of the Wire Scanner the maximum temperatures reached by the wire should be below of 3300 K, but the more important is the time during which the wire stays in this conditions.

# 10 Results

The different sets of simulation parameters have been used in order to test the calculation against the known experimental results and in order to predict the Wire Scanner operational limits for LHC. The parameters are summarized in Table 4. The beam parameters has been taken as nominal values, what is an example of what can be reached during the operation.

The conclusions concerning wire durability are drawn based on single experiment (SPS), in which the only measurement is the fact of the wire breaking in given beam conditions. Therefore the experiment is only an indication of the model validity, but has no statistical meaning.

## 10.1 SPS experiment in 1988

The model has been tested on the results of 1988 experiment on SPS beam. During this experiment the consecutive scans were performed with decreasing wire velocity. The wire has been broken at velocity of 10 cm/s [26] in beam conditions described in Table 4. At velocity of 20 cm/s the wire was still not broken, although it is possible that it was significantly weakened by the beam. Therefore the conditions present at

| variable name | unit | SPS | Main Injector | LHC inject. | LHC coll. |
|---|---|---|---|---|---|
| Physical parameters | | | | | |
| beam $\sigma_x$ | cm | 0.163 | 0.098 | 0.053 | 0.016 |
| beam $\sigma_y$ | cm | 0.065 | 0.098 | 0.080 | 0.023 |
| protons in beam | | $2 \cdot 10^{13}$ | $2 \cdot 10^{13}$ | $3.2 \cdot 10^{14}$ | $3.2 \cdot 10^{14}$ |
| fraction of the beam | | 1.0 | 1.0 | 0.25 | 0.065 |
| protons energy | TeV | 0.45 | 0.12 | 0.45 | 7 |
| wire velocity | cm/s | 10 | 691 | 100 | 100 |
| revolution time | s | $2.3 \cdot 10^{-5}$ | $1.1 \cdot 10^{-5}$ | $8.9 \cdot 10^{-5}$ | $8.9 \cdot 10^{-5}$ |
| No of protons passing wire | | $2 \cdot 10^{14}$ | $2 \times 1.7 \cdot 10^{13}$ | $2.7 \cdot 10^{13}$ | $7 \cdot 10^{12}$ |
| Numerical parameters | | | | | |
| $\Delta$x | cm | $3 \cdot 10^{-2}$ | $3 \cdot 10^{-2}$ | $1.5 \cdot 10^{-3}$ | $5 \cdot 10^{-4}$ |
| $\Delta$y | cm | 0.03 | 0.03 | 0.02 | 0.02 |

Table 4: *Values of parameters used in the calculations. The actual beam parameters in the position of the LHC Wire Scanners can vary depending on the version of the optics used. The* $\Delta$x *and* $\Delta$y *often vary for various runs, the values presented here are typical and the ones used to obtain presented results.*

the velocity of 10 cm/s cannot be taken as a threshold for safe use of the wire. A safety margin should be used.

During the scan with the wire speed of 10 cm/s the beam in the SPS has made about 4250 revolutions. The total energy deposited in the wire is about 0.3 J during the time of about 0.1 s, what gives an average power of about 3 W. The maximum heating power is about 7 W and this happens in t=50 ms after beginning of the scan when the beam center is reached. It is assumed that the effect of RF-heating during the scan is negligible for SPS fixed-target beam.

The temperature evolution of the central bin of the wire during the scan is visualized on the left plot of Figure 10. This plot is presents evolution for wire speeds of 10 cm/s (black line), 20 cm/s (blue line) and 100 cm/s (green line). The arrows show the moment when the wire passes the beam center.

For all velocities the maximum temperature is between 3500 and 3600 K. The fastest scan (green line) passes the center of the beam 4.9 ms after the beginning of the scan and the wire continues to absorb beam energy without a visible influence from cooling processes until it reaches the maximal temperature at 6.2 ms. Then it cools down fast by means of thermionic and radiative coolings. The period of high temperature lasts relatively short leading to the sublimation of 0.3% of the wire diameter.

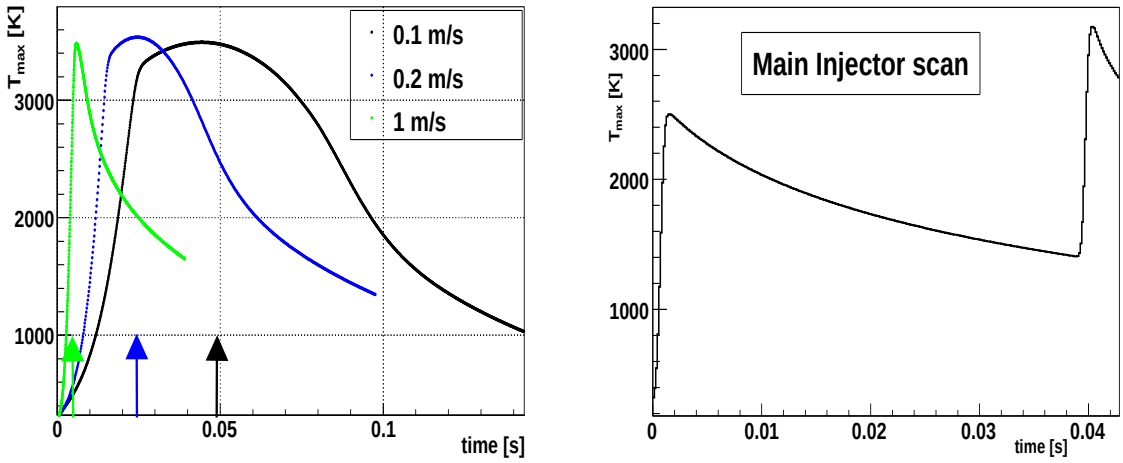


Figure 10: *Left plot: temperature of the central bin of the wire for 3 scan velocities: 10 cm/s (black curve), 20 cm/s (blue curve) and 100 cm/s (green curve). The arrows indicate moments when wire passes the center of the beam. Right plot: Evolution of the maximum temperature during the wire-destructive scan of Main Injector beam with rotational Wire Scanner with two passages of the wire through the beam.*

When the wire velocity decreases the situation looks different. For the scan with 10 cm/s, after 30 ms from the beginning, when the temperature of the wire reaches about 3200 K, the thermionic cooling process slows down the wire heating substantially. The maximum temperature is reached when the wire crosses the beam center at 49 ms from the beginning of the scan, but temperature change between 30 ms and 49 ms is small, pointing to a semi-equilibrium state between cooling and heating processes. The total energy deposited by the beam is 0.244 J and the total material sublimated is 7%.

As seen from above the experiment with SPS beam is particular. Time of scan is long enough to switch on the cooling processes, and as a result the wire center is heated to a temperature of about 3600 K for a time of about 40 ms.

It should be stated that the thermionic cooling is the main cooling mechanism in the above case. Therefore the poor knowledge of the carbon work function is an important source of uncertainty in the description of the process. If the work function is smaller by 20% (0.4 eV) then the maximal temperature drops down to about 3260 K and if it is by 20% higher (0.5 eV) the maximal temperature reaches 3740 K.

## 10.2 Wire Breakage in Main Injector of Tevatron

The rotative Wire Scanners on Tevatron's Main Injector pass the beam twice during the scan. The time between the two passes is about 40 ms therefore the wire has no time to cool down to initial temperature.

The beam parameters at which the wire damage occured has been recorded [27]. The wire linear speed was 691 cm/s but only a component perpendicular to the beam axis must be taken into account. The distance between the axis of the Wire Scanner rotation and the beam is 7 cm and the length of the fork arm is 13.5 cm. Therefore the effective velocity in the direction perpendicular to the beam is approximately 358 cm/s.

The maximum temperature evolution during this scan is presented in the right plot of Figure 10. The first peak reaches temperature of 2500 K and the second one 3180 K. The sublimation is negligible.

Most probably the wire got broken during the second passage through the beam. The conditions reproduced by the model are much less severe than in the case of SPS experiment. The are a few possible reason for this:

- A different wire types are used in CERN Wire Scanners and in Fermilab ones, therefore they have different thermomechanical properties.
- The wire history in the Main Injector is unknown and it could be that the wire has already been substantially weakened by the previous scans.
- In the rotational Wire Scanners an additional, centrifugal force is present during the scan; in case of Main Injector wire the additional acceleration was 353.7 m/s$^2$ ie. about 36 g, acting perpendicularly to the wire.

The predictions concerning the wire breakage on LHC presented in the following chapters are based on results of SPS experiment because a similar kind of Wire Scanner (linear) and similar wire will be used on LHC.

## 10.3 LHC injection beam

The LHC beam is much more dense than the SPS one. It contains 16 times more protons and the beam dimensions are smaller. The RF-heating from this beam can be substantial, especially that the wire can still stand a scan of a significant part of the beam. Therefore an initial temperature distribution shown on the right plot of Figure 8 is assumed.

During the scan the LHC bunches make 36 revolutions and the total energy deposited on the wire is 0.025 J in the time of about 3 ms what gives average heating power of almost 8 W.

The scan velocity is 1 m/s, which is the nominal wire velocity in LHC linear scanners. Even with this speed the wire heating from the full beam would destroy the wire immediately, therefore only a fraction of a full beam is considered in the calculations. This fraction is chosen in the way to reproduce maximum wire temperature of the safe scan know from SPS. Here this fraction is between 17% of the nominal beam current which gives 3300 K (safe for sublimation but conservative as seen from SPS experience) and 25% of the nominal beam current which gives already

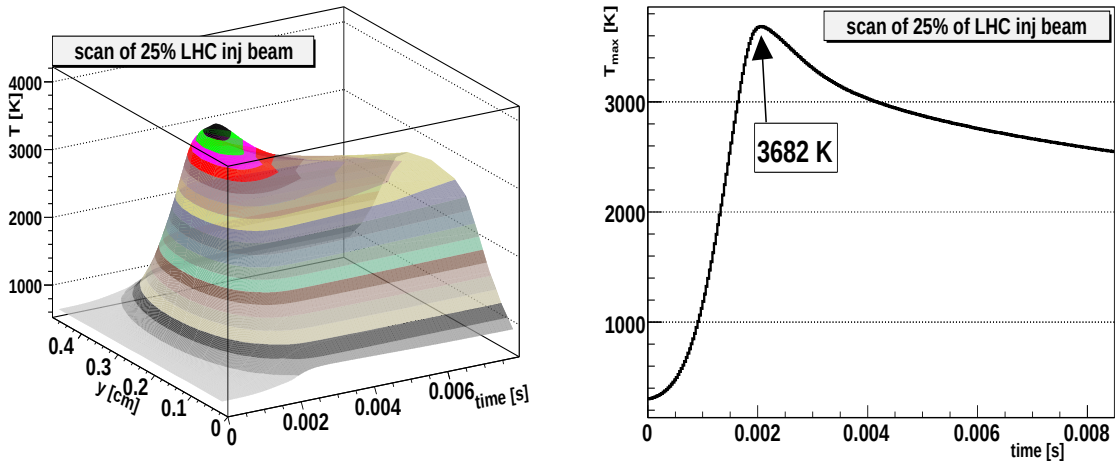


Figure 11: *Left plot: distribution of wire temperature during a scan of LHC injection beam with 25% of the nominal intensity. Right plot: the same but for the maximum temperature bin.*

3682 K (above the maximum temperature during wire-breaking scan but for much faster scan).

The maximum temperature evolution for the 25% of nominal beam can be traced on Figure 11. The beam maximum is reached after 1.6 ms but the temperature continues to raise until 2.1 ms reaching maximum of about 3682 K. The total material sublimated is about 0.5%.

## 10.4 LHC colliding beam

During the acceleration the LHC beam not only gains energy but also is squeezed by almost a factor 4 in each direction. The increase of beam energy leads to 10% decrease of energy deposited by a single proton as described in Section 3. The initial RF-heating is neglected as the maximum allowed beam current is expected to be small.

The scan velocity is 1 m/s and LHC makes only 11 revolutions during the scan of $3\sigma$ of the beam. In order to reach maximum wire temperature comparable to the safe scan in SPS, the beam intensity must be limited to only 5-7% of the nominal one. In such beam conditions the total energy deposited on the wire is 0.007 J during the time of about 1 ms what gives an average beam heating power of about 7 W.

In Figure 12 the temperature evolution during the scan of 6.5% of the LHC beam is presented. The beam center is reached after 0.48 ms and the maximum temperature of about 3683 K is reached 0.67 ms after the beginning of the scan. The total material sublimated in the hottest place of the wire is about 0.16% of the wire diameter. For the beam intensity limited to 5.3% of the nominal value the maximum temperature reached during the scan is 3320 K.

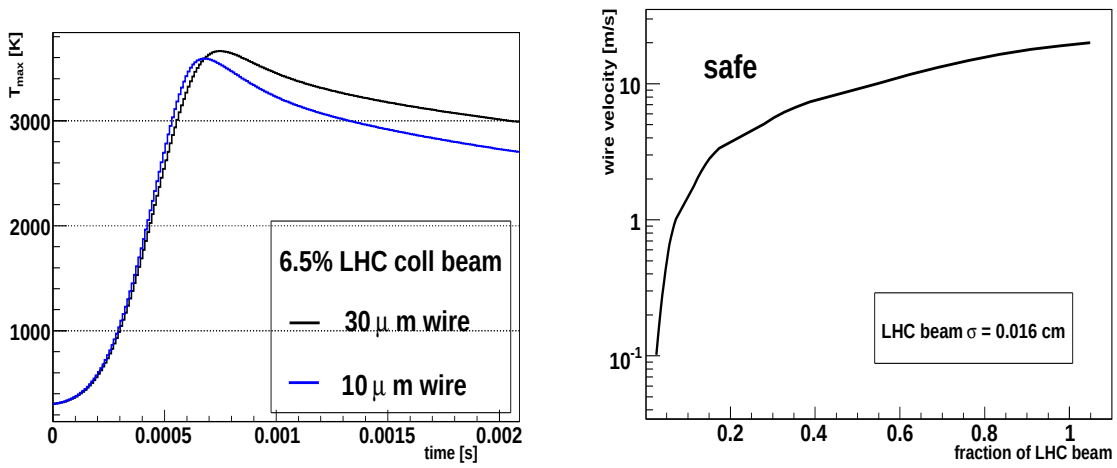


Figure 12: *Left plot: evolution of maximum wire temperature during the scan. Blue curve shows temperature evolution for* 10 $\mu$*m wire. Right plot: the region of safe operation of the Wire Scanner for LHC collision beam.*

A comparison of the temperature evolution for two wire diameters is made. The thinner wire reaches only slightly lower maximum temperature during the scan. This is because cooling effects, which are more efficient for a thinner wire due to better surface-to-volume ratio, have small impact on maximum temperature. However after the scan the thinner wire cools down much faster then the standard 30 $\mu$m one. One can conclude that use of a thinner wire, which is more difficult to handle, does not affect the scanner performance, but it should be reminded that it would produce smaller amount of secondary particles which are potentially dangerous for the superconducting magnets downward the scanner. In addition the thinner wires have typically better mechanical properties.

It is worth noticing that even for such a fast temperature increase, the thermo-mechanical shock should not be an important factor and should not affect the wire durability. The speed of sound in graphite is about $2.3 \cdot 10^5$ cm/s therefore during 0.5 ms when the wire temperature raises from 300 K to about 3670 K the elastic waves travel at distance of more than 1 meter. It can be concluded that the scan time is long enough to distribute the internal pressure change due to thermal shock smoothly along the wire.

# 11 Sensitivity to parameters

A test of the numerical stability of the simulation code has been done in order to assure the existing results and estimate errors of the numerical solution due to variation of program parameters. These tests show which parameters are crucial to perform a reliable estimation of temperature evolution during the scan process. They also show what physical phenomena are critical to Wire Scanner operation.

The results of the test are described in Table 5. The test has been performed for the case of LHC injection beam.

| Nr | variable | value | temperature [K] | remarks |
|---|---|---|---|---|
| 1 | carbon density $\rho_C$ [g/cm$^3$] | 1.8 | 3709 | |
| | | 2.0 | 3682 | |
| | | 2.2 | 3644 | |
| 2 | graphite emissivity $\epsilon$ | 0.6 | 3693 | poorly known |
| | | 0.8 | 3682 | |
| | | 1.0 | 3675 | |
| 3 | work function $\phi$ [eV] | 0.40 | 3403 | poorly known |
| | | 0.45 | 3682 | |
| | | 0.50 | 3916 | |
| 4 | variation of specific heat | $\times$0.9 | 3724 | |
| | | $\times$1.0 | 3682 | |
| | | $\times$1.1 | 3634 | |
| 5 | $N_{prot}^{total}$ | $6.4 \cdot 10^{13}$ | 3497 | 20% of nominal |
| | | $8 \cdot 10^{13}$ | 3682 | 25% of nominal |
| | | $9.6 \cdot 10^{13}$ | 3789 | 30% of nominal |
| 6 | bin size along the wire [cm] | 0.02 | 3688 | |
| | | 0.03 | 3682 | |
| | | 0.04 | 3673 | |
| 7 | bin size in direction of scan [cm] | 0.002 | 3681 | |
| | | 0.003 | 3682 | |
| | | 0.004 | 3687 | |

Table 5: *Results of variations of various parameters of numerical code.*

Variation of the carbon density by 10% leads to final temperature change of about 1%. The wire emissivity plays a negligible role in the final value of temperature. In contrary the variation of the work function by 10% leads to variation of temperature of the same order. This parameter is poorly known and it has a large impact on the wire temperature. Similarly a very important parameter, but for modelling of the sublimation process, is carbon vapour pressure.

The variation of the most important calculation parameters - bin size in direction of the wire and the size of the wire step, show good stability, therefore the algorithm used to solve the model is stable and the results it provides are reliable.

# 12 Conclusions

The model of the heating and cooling of the carbon wire inserted into particle beam has been constructed. The model has been verified on accessible data concerning wire temperature measurements and wire breaking conditions on LEP, SPS and Main Injector beams.

It has been found that scanning of LHC beams is a very fast process, therefore the cooling processes do not affect significantly the maximum wire temperature.

Assuming that the maximum temperature of the wire during the scan cannot significantly exceed value obtained in SPS wire breaking experiment (about 3600 K), it has been found that the wire will not break when scanning between 17 and 25% of the LHC injection beam and between 5 and 7% of the beam at collision. These values should be treated with safety factors due to the model uncertainties and because of the sublimation process which can weaken the wire without breaking it at the first scan. Increasing the wire speed to about 20 m/s, as presented on the right plot of Figure 12, would allow to scan full LHC beam at collision.

The other conclusions are the following:

- The thermionic current plays crucial role as a cooling process in temperatures above 3200 K, below that temperature the radiative cooling is dominant.
- RF-heating does not affect significantly the wire temperature in case of LHC beam (that means the heating from electronic energy deposition is much larger).
- The sublimation rate becomes significant for temperatures above 3300 K, but for fast scans of narrow, high-intensity beam the total amount of material sublimated during each scan is small.
- The heat transfer plays a minimal role as a cooling mechanism for high temperatures, therefore the eventual use of carbon nanotubes will not improve the Wire Scanner performance to scan stronger beams.
- The exact values of carbon work function and carbon vapour pressure are unknown and they are important parameters of the model.

It is not clear what kind of improvements can be made to increase the wire performance. A thinner wire is recommended because it usually has better mechanical properties and it reduces the number of particles hitting downstream magnet. An increase in the scan speed would decrease the amount of energy deposited in the wire and would allow to scan a higher fraction of the LHC beam. The chemical redeposition of sublimated carbon probably would not play an important role because LHC beams heat up the wire too fast.

The increase of the thermionic current could help to reduce the maximal temperature of the wire even during the scan of the most collimated beams. It could be done by introducing an additional electrode close to the beam. But the estimation of the electric tension needed to increase significantly the cooling is discouraging.

The comparison of wire breakage on SPS and on Main Injector of Tevatron might suggest that the rotational Wire Scanners impose more hard conditions on the wire during the scan than the linear ones. This might be due to the centrifugal force which acts perpendicularly to the wire axis during the scan.

A conclusion could be drawn that, as the LHC Wire Scanners work in critical conditions, probably the most valuable development would be to assure fast and automatic exchange of the broken wire and operate the most thin wires. A simple pre-cooling of the wire might increase the maximum beam intensity which can be scanned by a few percent.

# 13 Acknowledgments

I would like to thank Jan Koopman for encouraging me to make this study and for numerous discussions. Gianfranco Ferioli was very helpfull explaining the details of wire breakage conditions on SPS. Tom Kroyer has helped me to understand complexity of the electromagnetic field generated by the LHC beam. Special thanks to Martin Hu for useful discussions and for providing the Tevatron Main Injector beam parameters. Discussions with Delio Duarte Ramos gave me apprehension of mechanical properties of the wire. Last but not least I want to thank Bernd Dehning for his support and interest in this study and Barbara Holzer for careful reading of the manuscript.

# References

[1] K. Wittenburg, *Prepared for 39th ICFA Advanced Beam Dynamics Workshop on High Intensity High Bightness Hadron Beams 2006 (HB2006), Tsukuba, Japan, 29 May - 2 Jun 2006*

[2] F. Caspers, B. Dehring, E. Jensen, J. Koopman, J. F. Malo, F. Roncaloro, "Cavity Mode Related Wire Breaking of the SPS Wire Scanner and Loss Measurement of Wire Materials", CERN-AB-2003-067-BDI

[3] "Examen par MEB de cause de cassure de 2 fils torsads en carbone et de 3 fils neufs pour dtecteur de profils PS/Booster", CERN TS/MME-MM investigation report

[4] C.Field, D.McCormick, P.Raimondi, M.Ross, "Wire breakage in SLC wire profile monitors", SLAC-PUB-7832, May 1998

[5] J. M. Zazula, LHC Project Note 78/97

[6] J-B.Donnet, R.C.Bansal, "Carbon fibers", Marcel Dekker, New York (1990)

[7] Jan Koopman, private communication

[8] A.T.Dinsdale, "SGTE Data for Pure Elements", CALPHAD 15, 317-425 (1991)

[9] Y. S. Touloukian, R. W. Powell, C. Y. Ho and P. G. Klemens: Thermal Conductivity, Nonmetallic Solids, Thermophysical Properties of Matter (IFI/Plenum, New York, 1970), Vol. 2, (p. 6-46)

[10] W. M. Yao *et al.* [Particle Data Group], J. Phys. G **33** (2006) 1.

[11] B. Rossi, "High Energy Particles", Prentice-Hall, Inc., 1952.

[12] J. Bosser et al., "The micron Wire Scanner at the SPS", CERN SPS/86-26

[13] Michel Marie, private communication

[14] J.Carvalho, "Compilation of cross sections for proton-nucleus interactions at the HERA energy", Nucl.Phys.A725 (2003) 269-275.

[15] Report in prep.

[16] Vladimir Ivantchenko, private communication

[17] Y. S. Touloukian, R. W. Powell, C. Y. Ho and P. G. Klemens: Thermal radiative properties, nonmetallic solids Thermophysical Properties of Matter (IFI/Plenum, New York, 1970), Vol. 13, (p. 25)

[18] Delio Ramos et al., report in preparation

[19] S. Berber et al. "Unusally high thermal conductivity of carbon nanotubes", Phys. Rev. Lett. 2000, 84, 4613-4616

[20] Y. S. Touloukian, R. W. Powell, C. Y. Ho and P. G. Klemens: Thermal radiative properties, nonmetallic solids Thermophysical Properties of Matter (IFI/Plenum, New York, 1970), Vol. 8, (p. 6-46)

[21] H. Wiedmann, Particle accelerator physics, vol.2, Springer, 1995

[22] C. Fisher, R. Jung, J. Koopman, "Quartz wires versus Carbon fibres for improved beam handling capacity of the LEP Wire Scanners", CERN-SL-96-009-BI

[23] Tom Kroyer, "Simulation of Wire Scanner Heating by the Electromagnetic Field of a Particle Beam", CERN-AB-Note-2008-018

[24] P. Thieberger, "Upper Limits for Sublimation Losses from Hot Carbon Targets in Vacuum and in Gasses", MUC-0186, Brookhaven National Labolatory

[25] S. Grigoriev, E.Z. Meilikhov, "Handbook of Physical Quantities", CRC Press 1997, 324-337

[26] Gianfranco Ferioli, private communication

[27] Martin Hu, private communication